Atmospheric Measurement Techniques Discussions

Note on the application of planar-fit rotation for non-omnidirectional sonic anemometers

M. Li[1], W. Babel[2], K. Tanaka[3], and T. Foken[2,4]

[1]Cold and Arid Regions Environmental and Engineering Research Institute, Chinese Academy of Sciences, Lanzhou, China
[2]Department of Micrometeorology, University of Bayreuth, Bayreuth, Germany
[3]Hiroshima Institute of Technology, Hiroshima, Japan
[4]Member of Bayreuth Centre of Ecology and Environmental Research (BayCEER) of the University of Bayreuth, Bayreuth, Germany

Correspondence to: W. Babel (wolfgang.babel@uni-bayreuth.de)

Abstract

For non-omnidirectional sonic anemometers like the Kaijo-Denki DAT 600 TR61A probe, it is shown that separate planar fit rotations must be used for the undisturbed (open part of the sonic anemometer) and the disturbed sector. This increases the friction velocity while no effect on the scalar fluxes was found. In the disturbed sector, irregular values of $-\overline{u'w'} < 0$ were detected for low wind velocities. This study was done for data sets from the Naqu-BJ site on the Tibetan Plateau.

1 Introduction

The planar-fit method (Wilczak et al., 2001) was developed to allow for the use of the eddy-covariance technique in a heterogeneous landscape with a non-uniform wind field and to align the sonic anemometer with the streamlines of this wind field (Finnigan, 2004; Foken et al., 2012a; Rebmann et al., 2012). The rotation angles must be calculated for a long term data set of some weeks or months duration. This time period must be carefully determined depending on the structure of the underlying surface and the time of the year, including typical wind speeds and stratifications (Siebicke et al., 2012). The planar-fit rotation replaced the double rotation (Kaimal and Finnigan, 1994), which was normally applied on a single averaging period of about half an hour duration.

The planar-fit method is ideally suited for omnidirectional sonic anemometers like USA-1 (Metek GmbH), R3 (Gill Instruments Ltd.) and others. For these type of sensors no wind sector is significantly influenced by flow distortion, therefore the rotation follows the wind field and should not be affected by sonic anemometer structures. Nevertheless, an influence of such structures can also be found for omnidirectional sonic anemometers (Göckede et al., 2008), but often these are symmetric in three or four directions. This is not the case for sonic anemometers with an open measuring sector and a disturbed sector due to the anemometer mounting structure (Dyer, 1981). A classical representative of this anemometer type is the DAT 600 with the so-called

TR61A-probe, produced by Kaijo-Denki, Japan (Fig. 1a, Hanafusa et al., 1982), which is still in use. The most commonly currently used example is the CSAT3, produced by Campbell Scientific Ltd., USA (Fig. 1b).

The non-omnidirectional sonic anemometer has two sectors the disturbed sector and the undisturbed measuring sector with nearly no flow distortion. The undisturbed (open) sector extents from its centre ±60° for the Kaijo-Denki TR61A-probe (Fig. 1a), and ±170° in the case of the CSAT3 (Fig. 1b). The disturbed sector for CSAT3 was found to be approximately ±20° in wind tunnel measurements (Friebel et al., 2009). Field measurements typically show a standard deviation for wind direction of ±20°, which is also found in the data sets used for this study. To account for this, the undisturbed sector is assumed to be ±40° for DAT 600 and ±150° for CSAT3 in the following analyses. If the planar-fit rotation is applied for the complete data set the measurements in the undisturbed sector will be rotated due to the influence of the disturbed sector and the flux calculation will be based upon an erroneous mean vertical wind component. In the following, the possible effects will be discussed when routinely applying the planar-fit method (i.e. non-sector-wise) to non-omnidirectional sonic anemometers.

The Kaijo Denki sonic anemometer must normally be used together with a rotator and moved into the mean wind direction for each measuring series (Foken et al., 1988). If this is not done the results are significantly influenced in the 240° disturbed sector. A typical error is the occurrence of negative frictions $-\overline{u'w'} < 0$, (Gerstmann and Foken, 1984), where w' and u' are the fluctuations of the vertical wind component and the horizontal wind component, respectively, the latter is aligned into the mean wind direction. The anemometer is typically rotated into the mean wind direction and $-\overline{v'w'} \approx 0$ (v' wind component perpendicular to the mean wind direction). It follows for continuity reasons that $-\overline{u'w'} > 0$. A self-correlation, however, occurs between u' and w' due to flow distortion mainly in the case of low wind speeds, creating irregular friction values. Similar errors were also found in the data set of the CAMP/Tibet (Coordinated Enhanced Observing Period (CEOP), Asia-Australia Monsoon Project (CAMP) on the Tibetan Plateau) experiment (Li et al., 2006). Furthermore, for earlier experiments at

7325

this site in 1998 and 2002, Hong et al. (2004) reported about unclear differences of the wind measurements with the Kaijo Denki TR61A-probe and the CSAT3.

2   Material and methods

For this study, two well-analysed and data quality checked data sets from 6 February to 30 September 2008 (data set A) and from 14 May to 25 June 2010 (data set B), with half hour values of the calculated fluxes, were used. These data sets have been examined in preference to an earlier data set of CAMP/Tibet from 12 April 2004 to 3 September 2007 at the Naqu-BJ site (91° 48′ 59″ E, 31° 18′ 42″ N, 4502 m a.s.l.), where we already found negative friction for about 50 % of the data. Like during CAMP/Tibet, the Kaijo-Denki DAT 600 TR61A probe sonic anemometer was installed at 20 m height on a tower orientated to a westerly direction (270°, Fig. 1c) for data set A. Data set B also stems from the Naqu-BJ site, but was a direct comparison of the Kaijo Denki DAT 600 TR61A probe (orientation 263°) and the Campbell CSAT3 (orientation 213°) at a measuring height of 3.02 m (Fig. 1d). The Naqu-BJ site is located on the wide and level (incline < 2°) grassland (5 cm high during the monsoon season) near Nagqu city. The Nagqu area lies in the sub frigid climatic zone. The annual mean temperature ranges from −0.9 °C to −3.3 °C.

The data were analysed with the software package TK2/TK3 (Mauder and Foken, 2004, 2011; Mauder et al., 2008). This offers the possibility of applying the planar-fit method sector-wise within a given data set. The applied corrections were done in the software package according to Foken et al. (2012b).

The planar-fit method was applied for (i) the whole data set, and (ii) separately for the undisturbed and the disturbed sector. The undisturbed sector of the DAT 600 sonic anemometer was defined as ±40° from the centre of the undisturbed sector, for CSAT3 we used ±150°. Given the sensor orientation, the undisturbed sectors were identified for the DAT 600 from 230° to 310° (data set A) and from 223° to 303° (data set B). The remaining areas were treated as disturbed sectors. CSAT3 measurements are

7326

available only in data set B with a disturbed sector defined from 3° to 63°. Furthermore, the front sector from 183° to 243°, opposite to the disturbed sector, shows influence of CSAT3 sensor construction on the wind field. This sector was not excluded in the analysis, but a separate planar fit rotation was applied instead. The determination of the coefficients of the planar fit method was only done for such data classified as data with high or moderate quality (classes 1–6 according to Foken et al., 2004).

3 Results

Because the mean vertical wind velocity is mainly affected by flow distortion, these data are investigated in detail for both instruments and data sets. Figure 2 shows that the vertical velocity without any rotation for data set A is larger in the sector from 150° to 260° due to the higher wind speeds (Fig. 2a). After normalization with the mean horizontal wind velocity, the finding agrees with a tilt error and a sinuous-like w-values distribution (Fig. 2d). Singular and negative w-values were found for a wind direction of 140°, which is nearly identical to the tower position (Fig. 1c). For this analysis only data with high quality (classes 1–3 according to Foken et al., 2004) were used. By applying all data, the sinuous-like distribution can hardly be seen (not shown). The scatter around this distribution can be mainly attributed to data points where irregular friction occurs (red points in Fig. 2d). For data set B, smaller values occur due to the changed measurement height (Fig. 2b, c, e, f). After applying the planar-fit method for all wind directions, the vertical wind velocity is much smaller but still with a high scatter (Fig. 3a, b, c). For sector-wise planar fit, the undisturbed sector shows significantly lower vertical wind speeds of approx. $\pm 0.1\,\mathrm{m\,s^{-1}}$ for data set A (Fig. 3d). Only a small number of outliers are left with a higher-than-average occurrence of irregular friction. Significant scatter in the data can be found at 210° and 330°, corresponding to the anemometer construction (Fig. 1a), while the range from 120° up to 140° also includes the effects of the tower (Fig. 1c). Around 90° the data are affected due to the flow through the probe from behind. For data set B the results for DAT 600 are similar, and

also for CSAT3 the vertical wind velocity after rotation is reduced by the sector-wise planar fit, especially in the front sector (Fig. 3e, f).

Secondly, the data set was analysed regarding the condition $-\overline{u'w'} < 0$ for the planar fit rotated data. The result is illustrated in Fig. 4 and shows that irregular friction values in data set A are reduced by the sector-wise rotation in the optimal measuring sector (Fig. 4a, d). In the sector with flow distortion these values were only found for wind velocities below $6\,\mathrm{m\,s^{-1}}$ and in the non-neutral stability range. This is similar to the findings of Gerstmann and Foken (1984). Therefore, analogous to other sonic anemometers, the data of the undisturbed sector can be used with hardly any irregular friction velocities. This effect is obviously related to flow distortion, which is more significant for low wind velocities. An overview of the irregular data found in data set A is given in Table 1. For data set B, similar results for the DAT 600 were found (Fig. 4b, e) but many fewer occurrences of irregular friction velocity were found due to the low measuring height. Also, for CSAT3, data with $-\overline{u'w'} < 0$ are available mainly in the disturbed sector and for low data quality (Fig. 4c, f), and the sectorwise rotation reduces irregular friction, especially in the front sector (between the dashed lines). But more negative values remain in the front sector than in the surrounding ±30–90°. When no separate rotation for the front sector of the CSAT3 is made, however, there is nearly no difference visible between whole and sectorwise rotation (not shown). This suggests that the disturbed sector should be excluded but that the front and side sectors should be rotated separately.

The friction velocity and the sensible heat flux are compared when using only one rotation for the whole data set versus sectorwise rotation. The data of the disturbed sector was discarded. In Fig. 5 only data with high data quality (classes 1–3) are shown for data set A and DAT 600. When including moderate data quality (classes 4–6) the scatter is larger but the tendency of the regressions does not change (not shown). The friction velocity was improved through the sectorwise planar-fit rotation (Fig. 5, left), while the sensible heat flux was obviously not different for both planar-fit rotations (Fig. 5, right). The results for both data sets and instruments are shown in Table 2.

While the DAT 600 shows the same behavior in both data sets A and B, the friction velocity from CSAT3 is not significantly affected by the rotation method. This underlines the findings by Hong et al. (2004) for the Naqu-BJ site: "*There was little difference in kinematic sensible heat fluxes (not shown) [...] However, $\overline{u'w'}$ from KD was 5 % smaller than that from CS*" (KD: Kaijo Denki, CS: Campbell Scientific CSAT3). Hong et al. (2004) could not give an explanation for these differences and corrected the KD data with the CS measurements. Contrary to Hong et al. (2004), our findings for σ_u and σ_v showed no significant effect of the rotation method.

4 Conclusions

If non-omnidirectional sonic anemometers are not moved into the mean wind direction for each measuring series or the data are not selected only for the open sector of the anemometer, the coordinate rotation or planar-fit method must be applied with care. For the open sector of the anemometer a separate planar fit should be used. All data from the other sector must be flagged as low data quality, especially for low wind velocities irregular friction data are possible. The problem is not limited to the Kaijo Denki DAT 600 TR61A probe but is similar in the case of other sonic anemometer types, such as CSAT3 (Campbell Scientific Ltd.), with a much larger open sector of 340°. By applying the data quality schema according to Foken et al. (2004, Table 9.5, but not included in TK3 software) the data from the remaining disturbed sector of 20° (CSAT3) are flagged as containing errors (flag 9). But this selection must be applied before the planar fit rotation. Furthermore, the vertical wind velocity is also influenced by the CSAT3 probe supporting structures for wind directions from the front sector. A separate planar fit rotation for this sector substantially reduces mean vertical wind velocity and also has an effect on the friction velocity.

Published data of the Naqu-BJ site (Hong et al., 2004; Li et al., 2006) or other sites with Kaijo-Denki, TR61A-probe sonic anemometers should be used with care. Fortunately, only the friction velocity and standard deviations of the wind components

are affected, with no significant influence being found for scalar fluxes. Nevertheless, the separate planar-fit rotation should be used for all data. If the coefficients of the planar-fit rotation for both instruments were only determined for the undisturbed sector, differences in friction velocity between DAT 600 and CSAT3 can be substantially reduced (Table 3). Therefore a correction of DAT 600 data according to a comparison with a CSAT3, as done by Hong et al. (2004), does not seem to be necessary for high quality flux data from the undisturbed sector.

References

Dyer, A. J.: Flow distortion by supporting structures, Bound.-Lay. Meteorol., 20, 243–251, doi:10.1007/BF00119905, 1981. 7324

Finnigan, J. J.: A re-evaluation of long-term flux measurement techniques, Part II: Coordinate systems, Bound.-Lay. Meteorol., 113, 1–41, doi:10.1023/B:BOUN.0000037348. 64252.45, 2004. 7324

Foken, T., Zelený, J., Zubkovskij, S. L., and Fedorov, M. M.: Comparison of turbulence measuring instruments, in: Structure of the Boundary Layer over Non-Homogeneous Terrain, Proceedings of the Field Experiment KOPEX-86, Prague, 25–35, 1988. 7325

Foken, T., Göckede, M., Mauder, M., Mahrt, L., Amiro, B., and Munger, J.: Post-field data quality control, in: Handbook of Micrometeorology: a Guide for Surface Flux Measurement and Analysis, edited by: Lee, X., Massman, W., and Law, B., Kluwer, Dordrecht, 181–208, 2004. 7327, 7329, 7333, 7334, 7335, 7337, 7338, 7339

Foken, T., Aubinet, M., and Leuning, R.: The eddy covariance method, in: Eddy Covariance: a Practical Guide to Measurement and Data Analysis, edited by: Aubinet, M., Vesala, T., and Papale, D., Springer Atmospheric Sciences, Springer, The Netherlands, doi:10.1007/978-94-007-2351-1_1, 1–19, 2012a. 7324

Foken, T., Leuning, R., Oncley, S. R., Mauder, M., and Aubinet, M.: Corrections and data quality control, in: Eddy Covariance: a Practical Guide to Measurement and Data Analysis, edited by: Aubinet, M., Vesala, T., and Papale, D., Springer Atmospheric Sciences, Springer, The Netherlands, doi:10.1007/978-94-007-2351-1_4, 85–131, 2012b. 7326

Friebel, H. C., Herrington, T. O., and Benilov, A. Y.: Evaluation of the flow distortion around the Campbell scientific CSAT3 sonic anemometer relative to incident wind direction, J. Atmos. Ocean. Tech., 26, 582–592, doi:10.1175/2008JTECHO550.1, 2009. 7325, 7336

Gerstmann, W. and Foken, T.: Eigenschaften des Ultraschallanemometers der Firma Kaijo-Denki auf Grund der Ergebnisse von MESP-81 (Properties of the sonic anemometer of the Kaijo-Denki company on the basis of the results of the experiment ITCE-81), Geod. Geophys. Veröff., R. II, 26, 30–35, 1984. 7325, 7328

Göckede, M., Foken, T., Aubinet, M., Aurela, M., Banza, J., Bernhofer, C., Bonnefond, J. M., Brunet, Y., Carrara, A., Clement, R., Dellwik, E., Elbers, J., Eugster, W., Fuhrer, J., Granier, A., Grünwald, T., Heinesch, B., Janssens, I. A., Knohl, A., Koeble, R., Laurila, T., Longdoz, B., Manca, G., Marek, M., Markkanen, T., Mateus, J., Matteucci, G., Mauder, M., Migliavacca, M., Minerbi, S., Moncrieff, J., Montagnani, L., Moors, E., Ourcival, J.-M., Papale, D., Pereira, J., Pilegaard, K., Pita, G., Rambal, S., Rebmann, C., Rodrigues, A., Rotenberg, E., Sanz, M. J., Sedlak, P., Seufert, G., Siebicke, L., Soussana, J. F., Valentini, R., Vesala, T., Verbeeck, H., and Yakir, D.: Quality control of CarboEurope flux data – Part 1: Coupling footprint analyses with flux data quality assessment to evaluate sites in forest ecosystems, Biogeosciences, 5, 433–450, doi:10.5194/bg-5-433-2008, 2008. 7324

Hanafusa, T., Fujitani, T., Kobori, Y., and Mitsuta, Y.: A new type sonic anemometer-thermometer for field operation, Pap. Meteorol. Geophys., 33, 1–19, 1982. 7325, 7336

Hong, J., Choi, T., Ishikawa, H., and Kim, J.: Turbulence structures in the near-neutral surface layer on the Tibetan Plateau, Geophys. Res. Lett., 31, L15106, doi:10.1029/2004GL019935, 2004. 7326, 7329, 7330

Kaimal, J. C. and Finnigan, J. J.: Atmospheric Boundary Layer Flows: their Structure and Measurement, Oxford University Press, New York, NY, 1994. 7324

Li, M., Ma, Y., Ma, W., Hu, Z., Ishikawa, H., Su, Z., and Sun, F.: Analysis of turbulence characteristics over the Northern Tibetan Plateau area, Adv. Atmos. Sci., 23, 579–585, doi:10.1007/s00376-006-0579-z, 2006. 7325, 7329

Mauder, M. and Foken, T.: Documentation and Instruction Manual of the Eddy Covariance Software Package TK2, Work Report University of Bayreuth, Dept. of Micrometeorology, ISSN 1614-8916, 26, 42 pp., available at: http://opus.ub.uni-bayreuth.de/volltexte/2011/800/, 2004. 7326

Mauder, M. and Foken, T.: Documentation and Instruction Manual of the Eddy-Covariance Software Package TK3, Work Report University of Bayreuth, Dept. of Micrometeorology, ISSN 1614-8916, 46, 58 pp., available at: http://opus.ub.uni-bayreuth.de/volltexte/2011/866/, 2011. 7326

Mauder, M., Foken, T., Clement, R., Elbers, J. A., Eugster, W., Grünwald, T., Heusinkveld, B., and Kolle, O.: Quality control of CarboEurope flux data – Part 2: Inter-comparison of eddy-covariance software, Biogeosciences, 5, 451–462, doi:10.5194/bg-5-451-2008, 2008. 7326

Rebmann, C., Kolle, O., Heinesch, B., Queck, R., Ibrom, A., and Aubinet, M.: Data acquisition and flux calculations, in: Eddy Covariance: a Practical Guide to Measurement and Data Analysis, edited by: Aubinet, M., Vesala, T., and Papale, D., Springer Atmospheric Sciences, Springer, The Netherlands, doi:10.1007/978-94-007-2351-1_3, 59–83, 2012. 7324

Siebicke, L., Hunner, M., and Foken, T.: Aspects of CO_2 advection measurements, Theor. Appl. Climatol., 109, 109–131, doi:10.1007/s00704-011-0552-3, 2012. 7324

Wilczak, J., Oncley, S., and Stage, S.: Sonic Anemometer Tilt Correction Algorithms, Bound.-Lay. Meteorol., 99, 127–150, doi:10.1023/A:1018966204465, 2001. 7324

Table 1. Percentage of irregular data with $-\overline{u'w'} < 0$ for data set A (Kaijo Denki DAT 600 at 20 m height) for only the undisturbed sector and different data qualities according to Foken et al. (2004).

	Sectorwise planar fit		Whole planar fit	
Quality flag	Number of data	$-\overline{u'w'} < 0$	Number of data	$-\overline{u'w'} < 0$
1–3	964	20 %	920	34 %
1–6	1795	25 %	1766	43 %
1–8	2056	26 %	2056	46 %

Table 2. Regression analysis of the friction velocity and sensible heat flux according to $y = ax$ (the increment is in all cases nearly zero) with y for data with planar fit for the whole sector and x for data with planar fit for only the undisturbed sector (front sector of CSAT3 is included, but rotated separately) and different data qualities according to Foken et al. (2004).

Data set	Device	Quality flag	Friction velocity		Sensible heat flux	
			a	R^2	a	R^2
A	DAT 600	1–3	0.90	0.79	0.99	0.98
		1–6	0.88	0.74	0.97	0.95
B	DAT 600	1–3	0.93	0.99	0.99	0.99
		1–6	0.87	0.94	0.98	0.99
B	CSAT3	1–3	0.97	1.00	0.95	1.00
		1–6	0.96	0.99	0.95	0.99

Table 3. Regression analysis of the friction velocity and sensible heat flux according to $y = ax + b$ with planar fit for only the undisturbed sector (front sector of CSAT3 is included, but rotated separately) with y for DAT 600 and x for CSAT3 and different data qualities according to Foken et al. (2004).

Data set	PF rotation	Quality flag	Friction velocity			Sensible heat flux		
			a	b in $m s^{-1}$	R^2	a	b in $W m^{-2}$	R^2
B	sectorwise	1–3	0.96	0.003	0.95	0.94	3.14	0.92
		1–6	0.91	0.009	0.91	0.90	4.93	0.89
B	whole	1–3	0.90	0.004	0.94	0.93	4.01	0.92
		1–6	0.82	0.007	0.85	0.89	2.94	0.88
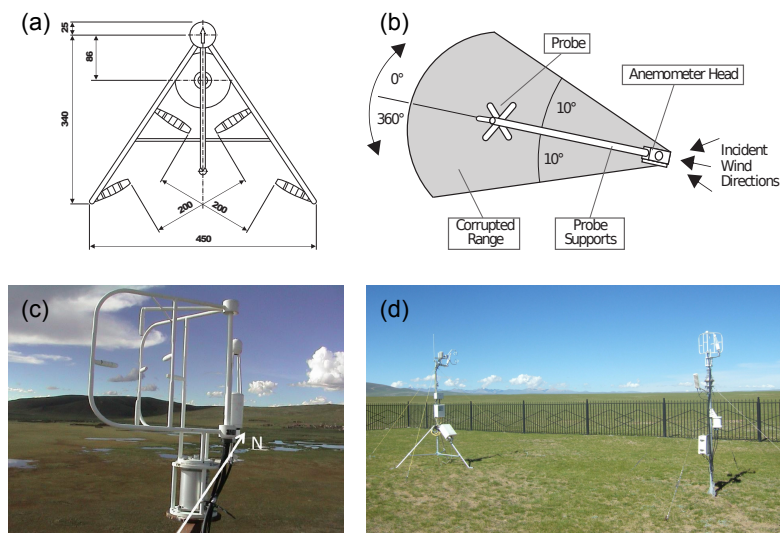
Fig. 1. (a) Kaijo-Denki, DAT 600, TR61A-probe, view from top (redrawn from Hanafusa et al., 1982). **(b)** Campbell CSAT3, view from top and orientation to north (Campbell Scientific Ltd., redrawn from Friebel et al., 2009); in accordance with wind tunnel measurements the disturbed sector is assumed to be smaller than in this study. **(c)** Kaijo-Denki, DAT 600, TR61A-probe installed at Naqu-BJ site at 20.8 m height on a 22 m tall tower with the open sector to west, data set A. The picture is taken from the perspective of the tower, the sonic measuring paths appear at an angle of roughly 320° (Photograph: Kenji Tanaka). **(d)** Campbell CSAT3 (left) and Kaijo Denki, DAT 600 TR61A probe (right) installed in 2010 at Naqu-BJ site at 3.02 m height with the open sector to west, data set B (Photograph: Tobias Gerken).
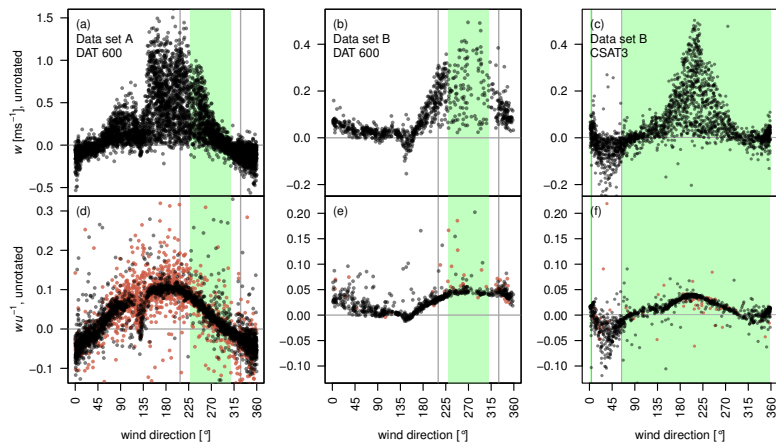
Fig. 2. Vertical wind velocity and its dependency on the wind direction for unrotated data and high data quality (flag 1–3 according to Foken et al., 2004); the upper row displays mean vertical velocity **(a–c)**, the lower row mean vertical wind velocity normalised by the horizontal wind velocity **(d–f)**; columns represent DAT 600, data set A on the left **(a, d)**, DAT 600, data set B in the middle **(b, e)** and CSAT3, data set B on the right **(c, f)**. The green sector is the undisturbed sector and the red points indicate data with $-\overline{u'w'} < 0$.
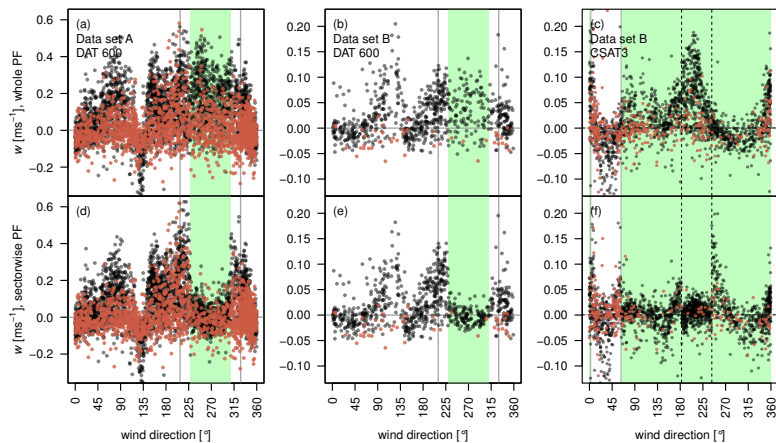
Fig. 3. Mean vertical wind velocity and its dependency on the wind direction for rotated data and high data quality (flag 1–3 according to Foken et al., 2004); the upper row displays mean vertical velocity rotated for the whole period **(a–c)**, the lower row mean vertical wind velocity rotated sectorwise **(d–f)**; columns represent DAT 600, data set A on the left **(a, d)**, DAT 600, data set B in the middle **(b, e)** and CSAT3, data set B on the right **(c, f)**. The green sector is the undisturbed sector and the red points indicate data with $-\overline{u'w'} < 0$; dashed lines for CSAT3 indicate the front sector, which is rotated separately.
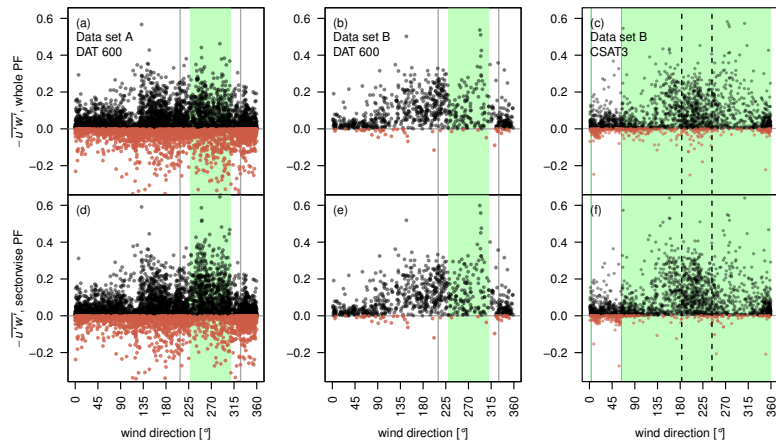
Fig. 4. Covariance $-\overline{u'w'}$ and its dependency on the wind direction for rotated data and high data quality (flag 1–3 according to Foken et al., 2004); The upper row displays $-\overline{u'w'}$, data rotated for the whole period **(a–c)**, the lower row $-\overline{u'w'}$, data rotated sectorwise **(d–f)**; columns represent DAT 600, data set A on the left **(a, d)**, DAT 600, data set B in the middle **(b, e)** and CSAT3, data set B on the right **(c, f)**. The green sector is the undisturbed sector and the red points indicate data with $-\overline{u'w'} < 0$; dashed lines for CSAT3 indicate the front sector, which is rotated separately.
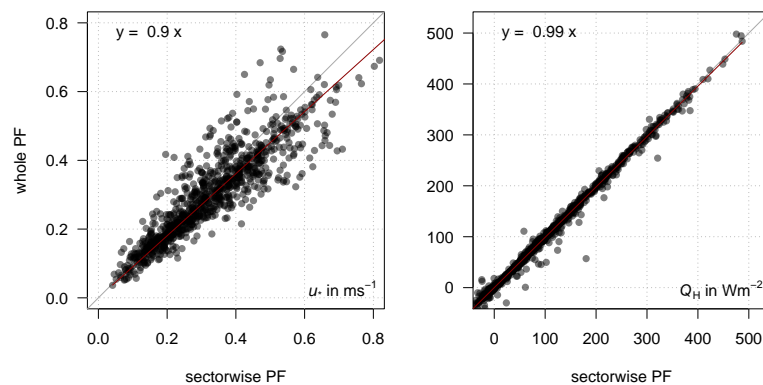
Fig. 5. Comparison of the friction velocity (left) and the sensible heat flux (right) with planar fit rotation for all wind directions and for sector wise planar-fit rotation and data quality 1–3 (data set A, DAT 600).